Brain Stimulation 16 (2023) 830–839

Contents lists available at ScienceDirect

Brain Stimulation

journal homepage: www.journals.elsevier.com/brain-stimulation

The timing of transcranial magnetic stimulation relative to the phase of prefrontal alpha EEG modulates downstream target engagement

Spiro P. Pantazatos [a,1], James R. Mclntosh [b,c,1], Golbarg T. Saber [d,e,1], Xiaoxiao Sun [b], Jayce Doose [f], Josef Faller [b], Yida Lin [g], Joshua B. Teves [d], Aidan Blankenship [d], Sarah Huffman [i], Robin I. Goldman [j], Mark S. George [i,k], Paul Sajda [b,h,l,m,*], Truman R. Brown [f,g,**]

[a] Department of Psychiatry, Columbia University Irving Medical Center, New York, NY, 10027, USA
[b] Department of Biomedical Engineering, Columbia University, New York, NY, 10027, USA
[c] Department of Orthopedic Surgery, Columbia University Irving Medical Center, New York, NY, 10032, USA
[d] Department of Radiology and Radiological Science, Medical University of South Carolina, Charleston, SC, 29425, USA
[e] Department of Neurology, University of Chicago, Chicago, IL, 60637, USA
[f] Center for Biomedical Imaging, Medical University of South Carolina, Charleston, SC, 29425, USA
[g] Department of Computer Science, Columbia University, New York, NY, 10027, USA
[h] Department of Radiology, Columbia University Irving Medical Center, New York, NY, 10032, USA
[i] Department of Psychiatry and Behavioral Sciences, Medical University of South Carolina, Charleston, SC, 29425, USA
[j] Center for Healthy Minds, University of Wisconsin-Madison, Madison, WI, 53705, USA
[k] Ralph H. Johnson VA Medical Center, Charleston, SC, 29401, USA
[l] Department of Electrical Engineering, Columbia University, New York, NY, 10027, USA
[m] Data Science Institute, Columbia University, New York, NY, 10027, USA

ARTICLE INFO

Keywords:
Neurostimulation
DCM
Dynamic causal modeling
Target engagement
Transcranial magnetic stimulation
Electroencephalogram

ABSTRACT

Background: The communication through coherence model posits that brain rhythms are synchronized across different frequency bands and that effective connectivity strength between interacting regions depends on their phase relation. Evidence to support the model comes mostly from electrophysiological recordings in animals while evidence from human data is limited.

Methods: Here, an fMRI-EEG-TMS (fET) instrument capable of acquiring simultaneous fMRI and EEG during noninvasive single pulse TMS applied to dorsolateral prefrontal cortex (DLPFC) was used to test whether prefrontal EEG alpha phase moderates TMS-evoked top-down influences on subgenual, rostral and dorsal anterior cingulate cortex (ACC). Six runs (276 total trials) were acquired in each participant. Phase at each TMS pulse was determined post-hoc using single-trial sorting. Results were examined in two independent datasets: healthy volunteers (HV) (n = 11) and patients with major depressive disorder (MDD) (n = 17) collected as part of an ongoing clinical trial.

Results: In both groups, TMS-evoked functional connectivity between DLPFC and subgenual ACC (sgACC) depended on the EEG alpha phase. TMS-evoked DLPFC to sgACC fMRI-derived effective connectivity (EC) was modulated by EEG alpha phase in healthy volunteers, but not in the MDD patients. Top-down EC was inhibitory for TMS pulses during the upward slope of the alpha wave relative to TMS timed to the downward slope of the alpha wave. Prefrontal EEG alpha phase dependent effects on TMS-evoked fMRI BOLD activation of the rostral anterior cingulate cortex were detected in the MDD patient group, but not in the healthy volunteer group.

Discussion: Results demonstrate that TMS-evoked top-down influences vary as a function of the prefrontal alpha rhythm, and suggest potential clinical applications whereby TMS is synchronized to the brain's internal rhythms in order to more efficiently engage deep therapeutic targets.

* Corresponding author. Department of Biomedical Engineering, Columbia University, New York, NY, 10027, USA.
** Corresponding author. Center for Biomedical Imaging, Medical University of South Carolina, Charleston, SC, 29425, USA.
E-mail addresses: psajda@columbia.edu (P. Sajda), brotrr@musc.edu (T.R. Brown).
[1] Contributed equally.

https://doi.org/10.1016/j.brs.2023.05.007
Received 7 September 2022; Received in revised form 26 April 2023; Accepted 8 May 2023
Available online 13 May 2023

1. Introduction

Data from animal studies show that brain rhythms are synchronized across different frequency bands and are highly structured across areas, layers and their corresponding projections [1]. In the communication through coherence model, cognition relies on patterns of neural synchronization that change dynamically with stimulation and behavioral context [1,2]. The model proposes that bottom-up-directed gamma band influences are controlled by top-down-directed alpha-beta band influences, and that rhythmic modulation of postsynaptic excitability and coherence between pre- and postsynaptic neuronal groups are the basis for strong effective connectivity [1]. Moreover, the effective connectivity strength between interacting regions may depend on their phase relation, as suggested by recordings in visual cortex of awake cats and monkeys [3]. However, there is limited human data in support of this model as a principle for top-down influences and dynamic network coupling. An inherent challenge in acquiring such data is the need for non-invasive, spatiotemporal measurements of distributed brain activity. With respect to brain stimulation, if methods for acquiring such data in humans could be developed, then one could imagine using them to advance both basic and clinical neuroscience. For example, perturbation-based neuroimaging systems could be used to advance our understanding of basic cognitive neuroscience via probing of directed dynamics and causal interactions of neural networks. Clinically, such methods could be used to individualize neurostimulation to maximize target network engagement for treating diseases such as depression.

EEG, fMRI, and transcranial magnetic stimulation (TMS) have been used together in a pair-wise fashion to non-invasively investigate brain networks, and the feasibility of concurrent fMRI-EEG-TMS (fET) with offline analysis of results has been previously demonstrated [4]. We have created a system of simultaneous fET, where the timing of TMS delivery relative to the EEG signal can be determined. This enables assessment of EEG phase-dependent TMS effects on brain activity. Importantly, it would allow us to test whether TMS that is synchronized to the brain's internal cortical rhythms has differential effects on deeper corticolimbic brain structures involved in emotion processing and regulation. If so, this could facilitate clinical applications. For example, TMS could be timed to optimize therapeutic engagement of the anterior cingulate cortex (ACC) in patients with major depressive disorder (MDD).

Neural oscillations in the alpha band (8–12 Hz) are viewed as an active inhibitory mechanism that gates and controls information processing depending on task demands [5], and global synchrony in the (upper) alpha band may subserve resting-state BOLD activity in the (task-positive) fronto-parietal network related to cognitive control and attention [6,7]. While alpha activity can be predominantly recorded from the occipital lobes at rest with eyes closed, EEG recordings of alpha at F3 reflect neural activity that is distinct from occipito-parietal activity (see Supplementary Information S.10 in Ref. [8]). Previous studies have shown that the timing of stimulus onset relative to the phase of the alpha cycle influences perception [9–11], suggesting alpha phase could potentially act as a gating mechanism where different phases in the cycle are associated with states of low and high excitability within the network.

Previous research using simultaneous TMS-EEG has demonstrated that motor excitation following TMS pulses varies with EEG phase and amplitude [12–15]. Using simultaneous EEG-fMRI, our group has previously shown that BOLD activity in decision related networks were modulated by the prestimulus EEG alpha phase during an auditory oddball task [16]. Based on these previous findings, we hypothesized that single pulse TMS stimulation to left DLPFC synchronized with respect to alpha phase would modulate ACC functional and effective connectivity with the left DLPFC as well as ACC activation.

Here, fET was used to determine whether TMS delivered to DLPFC at different phases of the alpha cycle modulated functional and effective connectivity with ACC. Whether alpha phase at TMS pulse onset modulated ACC BOLD activity was also examined. We examined single pulse TMS during a task-free, resting state design for two main reasons: global synchrony in the (upper) alpha band has been previously shown to underlie resting-state BOLD activity in the (task-positive) fronto-parietal network related to cognitive control and attention [6,7], and also to mirror the task-free design that was done during the rTMS therapy sessions in a subset of subjects undergoing treatment [8]. Our fET instrument can acquire simultaneous fET and remove fMRI artifacts from the EEG automatically in real-time [17]. Offline analyses were used to recover the exact phase of alpha at each single pulse TMS onset via causal signal processing. Being able to observe changes in the level of connectivity and activity in the ACC following a TMS pulse that is timed to EEG cortical rhythm may lead to optimizations in TMS timing that could have better clinical efficacy than current, non-synchronized TMS approaches.

We focused our study on the ACC (see ClinicalTrials.gov ID: NCT03421808) and more specifically three subregions of ACC (dorsal ACC, or dACC; rostral ACC, or rACC, and subgenual ACC, or sgACC) and their TMS-evoked functional connectivity with DLPFC based on previously established functional or structural connectivity between these ACC subregions with DLPFC and their relevance to TMS treatment of depression and related symptomatology [18–21]. A psychophysiological interactions (PPI) [22,23] analysis was used to estimate and compare correlations between two regions' (nuisance adjusted) BOLD time courses as a function of condition (i.e. TMS pulses during one of four alpha phase bins). This analysis was chosen to test for phase dependence of TMS-evoked brain functional connectivity (FC) given the importance of functional connectivity between DLPFC and sgACC in determining TMS outcomes [19,21]. Significant PPI findings were further interrogated with Dynamic Causal Modeling (DCM) and model selection to test for evidence of top-down TMS-evoked effective connectivity between DLPFC and sgACC and to test whether the estimated connectivity strengths vary as a function of prefrontal alpha phase at TMS pulse onset.

2. METHODS

Due to space constraints, full methods are presented in detail as supplementary information (SI) in the supplement. Briefly, results from two independent datasets (cohorts) are presented in the current study: the primary dataset consisted of healthy volunteers (HV, N = 11), and a second dataset was comprised of patients with major depressive disorder drawn from an interim blinded analysis of an ongoing clinical trial (MDD, N = 17). See SI sections S.1.1 and S.1.2 for sample details including inclusion and exclusion criteria. The second dataset was used to test generalizability of the findings in the primary dataset, and not to make direct comparisons between HV and MDD.

Each subject in the study underwent fMRI and EEG scanning while receiving single-pulse TMS neurostimulation using a simultaneous 3-way fET acquisition system developed by our group and previously described in Ref. [17]. Each subject, except for 3 HV subjects, received 6 sessions of fET scanning, and 46 TMS pulses were delivered per session. Three HV subjects had 1 or 2 sessions discarded due to system malfunctions. The instrument included a custom 43 channel MR compatible bipolar EEG system (Innovative Technologies, CA, USA) described in Refs. [24,25], a Siemens 3T Prisma MRI Scanner using a custom 12 channel head coil (Rapid MR International), and a MagStim Rapid2 TMS neurostimulator with a modified MRI-compatible TMS coil. Functional imaging was performed with a custom 12-channel head coil (Rapid MR International, LLC, Columbus, OH, USA) and a multi-echo multiband pulse sequence (CMRR, University of Minnesota) while EEG was simultaneously acquired at 488 Hz sampling rate using an MR compatible bipolar EEG cap with 36 electrodes placed on the subject's head. The montage is a hardwired bipolar EEG cap designed to minimize the induced electromagnetic interference from the MR and TMS fields [24]. The location of the DLPFC was measured and marked (under the

F3 electrode) for TMS coil placement in the MRI scanner. We used the Beam F3 locator to mark the EEG F3 [26] location in DLPFC of each subject consistent with recent consensus guidelines [26–28]. Full details of fET acquisition and scanning parameters are described in SI S.1.3.

The EEG data was corrected for TMS and gradient artifact, and then rereferenced from a bipolar to a unipolar referencing scheme (see Ref. [24] and SI S.1.4 for more details). The phase of the alpha oscillation φ_α at the trigger time of a TMS pulse was then estimated with a machine learning approach that produces causal estimates of the instantaneous phase from the raw signal [29] (see S.1.4.3 for details).

For fMRI analysis, three regions (dorsal, rostral and subgenual ACC) were defined and used for ROI functional connectivity and activation analysis. Dorsal ACC (dACC) and rostral ACC (rACC) anatomical masks were generated from freesurfer in AFNI for the left and right dorsal (caudal) and rostral (ventral) ACC. The subgenual ACC (sgACC) ROI was generated using a 10 mm sphere centered at MNI = [6 16 -10] and excluding white matter as previously described in Ref. [19]. This location corresponds to the MNI coordinate that is most responsive to interventions for depression averaged across multiple studies [19], and is also anticorrelated with various TMS DLPFC target sites at rest [21]. The T2-weighted fMRI data were preprocessed using SPM12 (see SI S.1.5 for more details).

Our primary statistical analysis tested whether TMS-evoked functional connectivity (FC) between the left DLPFC stimulation site and ACC depended on alpha phase at TMS pulse onset using a generalized Psychophysiological Interactions analysis (PPI) [22,23], see SI S.1.5.3. We then interrogated the direction and phase-dependent dynamics of coupling between the left DLPFC and sgACC using Dynamic Causal Modeling (DCM) for SPM12 (see SI S.1.5.4). Our secondary analyses tested for phase-dependent TMS-evoked BOLD activation in the ACC using both conventional SPM (GLM) ROI analysis as well as generalized additive mixed models (GAMM, see SI S.1.5.5). Note that all analyses except for the GAMM grouped together TMS pulse onsets into four separate phase bins. Phase binning allowed for the use of more conventional approaches (i.e. 1-way ANOVA, GLM, PPI and DCM) at the expense of averaging away signal within each phase bin. The GAMM model overcomes this limitation at the expense of higher model complexity.

3. RESULTS

3.1. Functional connectivity between DLPFC and sgACC depends on EEG alpha phase

The overall study design and analysis workflow is outlined in Fig. 1. Given the importance of resting-state FC between the DLPFC TMS stimulation site and sgACC in determining depression treatment outcomes [19,21], our main statistical analysis tested whether TMS-evoked DLPFC-sgACC FC is moderated by prefrontal alpha EEG phase. Throughout the study, phase angles are expressed in relation to a cosine (i.e. 0° is the peak) consistent with related studies of phase-locked TMS delivery [30]. Generalized psychophysiological Interactions (PPI) analysis (see SI S.1.5.3) was applied with phase bin as the "psychological" condition-of-interest, and TMS pulse onsets were grouped into one of four conditions according to phase bin (bin 1: $-\pi$ to $-1/2\ \pi$, bin 2: $-1/2\ \pi$ to 0, bin 3: 0 to $1/2\ \pi$, and bin 4: $1/2\ \pi$ to π). Below we present results using both conventional ROI analyses as well as small volume correction which is sensitive to weaker, spatially distributed signal within each ROI.

ROI analysis: When applying an ROI analysis (averaging signal within each of 5 ROIs: sgACC and left and right rACC and dACC), alpha phase at TMS pulse onset moderated DLPFC-sgACC functional connectivity in both datasets (**HV**: $F_{3,40} = 3.07$, $p = 0.038$ uncorrected; **MDD**: $F_{3,64} = 3.2$, $p = 0.029$ uncorrected; Fisher's combined $p = 0.009$), but not DLPFC-dACC or DLPFC-rACC functional connectivity (see Fig. 2, top row). To further interrogate the results a permutation approach was applied whereby SPM.mat design files (TMS phase conditions) were shuffled across subjects and followed by the same ROI analysis. The resulting p-values were consistent with ROI analysis results (**HV** $p = 0.02$; **MDD** $p = 0.02$; Fisher's combined $p = 0.004$).

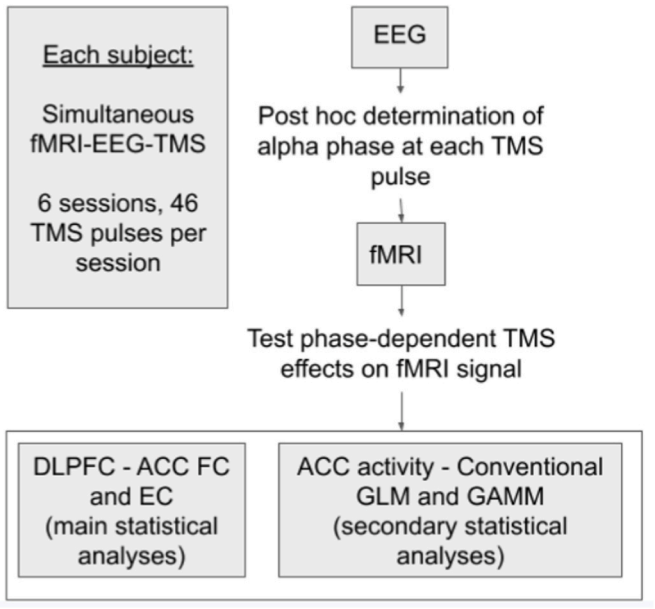

Fig. 1. Overall study design and analysis flow. Simultaneous fMRI and EEG were acquired from each subject during single pulse TMS delivery (6 sessions per subject, 46 TMS pulses per session). After preprocessing, the EEG signal was used to estimate the alpha phase at each TMS pulse. This information was then used in the fMRI analysis to test for phase-dependent effects of TMS on DLPFC-ACC functional and effectivity connectivity (main statistical analyses) and on ACC activity (secondary statistical analyses.

Small Volume Correction: In addition to conventional ROI analysis (where signal within each mask is averaged together), a voxel-wise analysis within each ACC mask was applied using the mask for small volume correction. Consistent with the ROI analysis results, alpha phase bin at TMS pulse onset moderated functional connectivity between the DLPFC TMS target site and sgACC in the **HV** dataset (voxel-wise FWE corrected $p = 0.068$, cluster-extent corrected $p < 0.05$). The results from 3dClustSim (compiled December 11, 2018) were confirmed using non-parametric permutation (FSL v5.0 randomise function) with 2000 permutations and a CDT of $F = 2.75$ (equivalent to $p = 0.01$ uncorrected for F with [3,64] degrees of freedom). Exchangeability blocks (i.e. subjects) were provided to the algorithm so that phase bin parameter estimates were permuted within each subject given they are not independent measures. The results confirm a significant effect of alpha phase bin on DLPFC-sgACC FC (first dataset and second dataset cluster-extent corrected $p = 0.0035$ and $p = 0.0085$, respectively, and Fisher combined p-value = 0.00035). A voxel-wise analysis was also conducted using the same cluster-determining threshold ($p = 0.01$ uncorrected) to test for brain-wide effects of phase bin on activation analysis (standard GLM approach) and TMS-evoked functional connectivity with DLPFC. Neither analysis yielded significant clusters at $p < 0.05$ cluster-extent corrected (data not shown) when using 3dClustSim (compiled December 11, 2018) or FSL v5.0 randomise.

Note that our use of a cluster-determining threshold (CDT) of p = 0.01 is unlikely to result in false positives in our analysis because we use an ROI approach. Eklund et al. [31] was concerned with CDT and false-positive rates using whole-brain cluster-extent correction. Eklund et al. also concluded that permutation-based approaches (i.e. FSL randomise) have acceptable false positive rates, and our results were more significant when permutation-based approach (FSL randomise) was applied (the p-values for DLPFC-sgACC FC were one order of magnitude

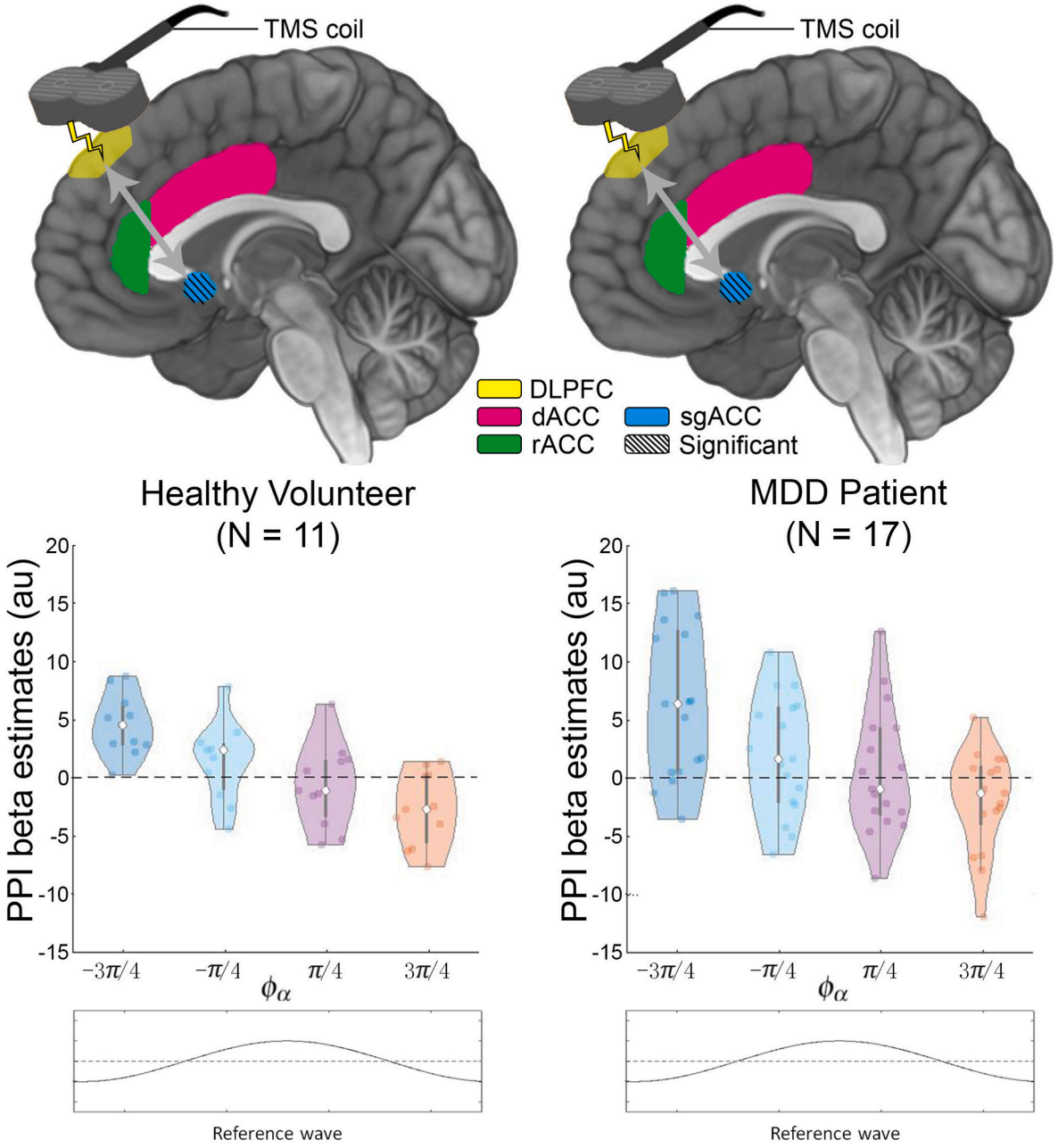

Fig. 2. Alpha phase at TMS stimulation moderates functional connectivity between DLPFC (EEG F3) and subgenual anterior cingulate cortex (sgACC). Generalized psychophysiological interactions analysis (PPI) was used to estimate TMS-evoked DLPFC-sgACC functional connectivity within each of four alpha phase bins. The voxel-wise analysis was restricted to a search space within a subgenual ROI generated using a 10 mm sphere centered at MNI = [6 16 -10] and excluding white matter as in Ref. [19]. A group level omnibus F-test on the beta weight parameter estimates (PE) identified a cluster in the primary dataset ($p < 0.05$ corrected, left). The findings replicated in the second independent cohort ($p < 0.05$ corrected, right). The bottom row shows violin plots of PEs averaged within clusters (contiguous voxels surviving $p < 0.05$ uncorrected).

smaller than 3dClustSim).

A cluster within the sgACC ROI search region was defined using an F-test thresholded at $p < 0.05$ un-corrected, then used to visualize and plot the beta parameter estimates for each of the four phase bins across subjects. The functional connectivity between DLPFC and sgACC was highest (most positive) when the TMS pulse occurred during the rising phase of the alpha oscillation in bins 1 and 2 ($-3/4\pi$ and $-1/4\pi$), and the lowest (negative) during the falling phase in bins 3 and 4 (centered at $1/4\pi$ and $3/4\pi$, respectively, see Fig. 2, bottom left). This finding replicated in the **MDD** dataset (voxel-wise FWE corrected $p = 0.037$, cluster-extent corrected $p < 0.05$, see Fig. 2, bottom right). The greatest pairwise difference, consistent across both datasets, was between phase bin 1 vs. bin 4: DLPFC−sgACC functional connectivity was highest in bin 1 and lowest in phase bin 4 (**MDD**: $t_{64} = 4.4$, FWE voxel-wise corrected $p = 0.004$, cluster extent corrected $p < 0.05$).

We tested whether results are sensitive to phase bin center selection by repeating the analysis with phase bin centers shifted by 45°. In this analysis, no effect of phase bin was observed, likely because the signal was diluted by averaging events from adjacent phase bins with the highest and lowest PPI beta estimates (see SI S.2).

3.2. Top-down DLPFC-sgACC effective connectivity depends on EEG alpha phase

Functional connectivity results indicate there is a statistical association between fMRI BOLD activity in ACC and DLPFC that depends on alpha phase, but they do not enable inference about the direction of information flow between the two areas. To infer causal influences between DLPFC and ACC in response to TMS, as a function of alpha phase, a simple dynamic causal model (DCM) of DLPFC and sgACC was estimated for each subject. The DCM modeled experimental modulation (TMS) of both extrinsic (i.e. between-region) and intrinsic (i.e. self or within-region) connections during each of four phase bins (see section 3.1). A form of Bayesian Model Comparison and Reduction [32] was applied to compare the full model to 'reduced' versions of the model along three factors: TMS modulation of top-down vs bottom up extrinsic connectivity, TMS modulation of DLPFC vs sgACC intrinsic connectivity, and TMS as driving input to DLPFC vs sgACC (see Figure S1A in SI). The full DCM model is represented by the 1st model along each factor shown in Figure S1A in SI. This created a search space of 64 unique models. The average 'baseline' effective connectivity (EC), or bidirectional connectivity representing the mean across all TMS phase conditions or during baseline in non-centered models, *A* matrix in the DCM [33], was included in all models (see SI S.1.5.4). Note that the term "modulate" is used here in the same way it is used in the DCM for fMRI literature: as in an experimental condition may "modulate" self-connections, connections between regions, and/or activity of a region itself. The term is not used to suggest the induction of synaptic plasticity (i.e., short-term and long-term plasticity).

Model evidence was summed across all models belonging in each level, or 'family' of models, for each factor (Figure S.1B in SI). In the **HV** dataset, results suggest a model in which TMS modulates intrinsic connectivity of both DLPFC and sgACC as well as both bottom-up and top-down connectivity between the two regions, while TMS does not directly drive activity in either region. In the **HV** dataset, the average top-down effective connectivity (EC) was excitatory (i.e. the *A* matrix parameter was positive with significant posterior probability $P_p > 0.95$), and the bottom-up EC was inhibitory (negative *A* matrix parameter, $P_p > 0.95$), while in the **MDD** dataset, both the top-down and bottom-up average EC were excitatory (Fig. 3A). In the **HV** dataset, the top-down EC was modulated by TMS alpha phase (uncorrected $p < 0.001$), while trend-level evidence suggested intrinsic sgACC connectivity was modulated by alpha phase at TMS pulse onset in both datasets (Fig. 3A). The DLPFC-

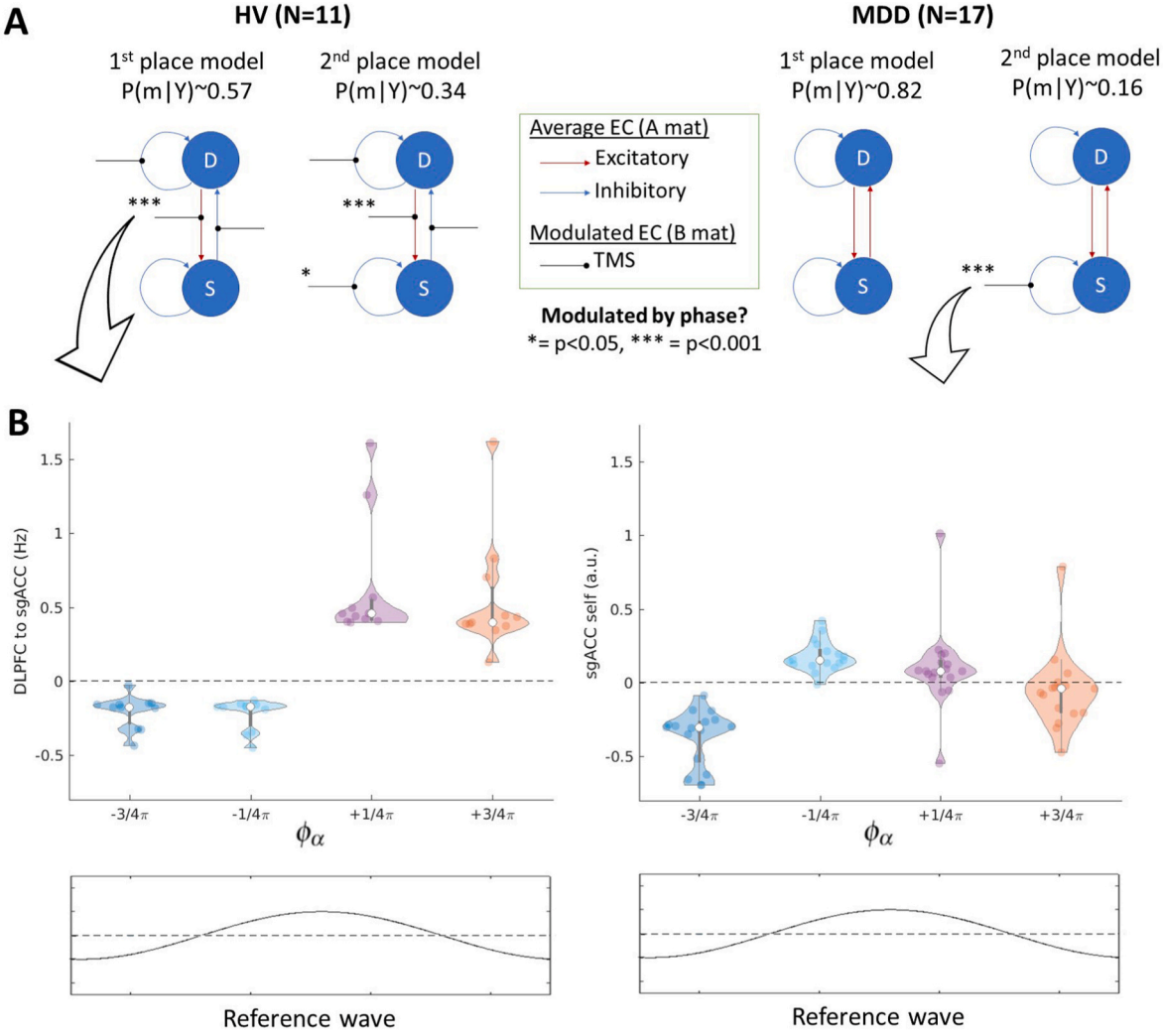

Fig. 3. Dynamic causal modeling suggests TMS-evoked top-down DLPFC-sgACC effective connectivity (EC) depends on EEG alpha phase. **A)** The top 2 winning network structures from Bayesian Model Comparison (see methods) are shown in each dataset. EC strengths that were modulated by alpha phase at TMS pulse onset are shown with asterisks (* indicates $p < 0.05$ uncorrected, *** indicates $p < 0.001$ uncorrected). Results suggest prefrontal alpha phase moderates TMS-evoked DLPFC-sgACC top-down EC in HV, but not in MDD. B) Violin plots in HV show top-down EC is inhibitory during the rising phase of alpha, and excitatory during the falling phase. In MDD, the DCM results suggest alpha phase at TMS pulse onset moderates intrinsic (self) sgACC connectivity, with the lowest parameter values (excitatory effects) during the initial rising phase of the alpha wave. See Figure S1 in SI for network model space and model comparison results.

sgACC EC results in HV were confirmed using a non-parametric permutation analysis, whereby the DCM and repeated measures ANOVA were re-estimated 50 times after randomly permuting phase bin labels with respect to each subject's fMRI data. In this analysis, no F-value in the null distribution was higher than the F-value that resulted from unshuffled data ($p < 0.01$, data not shown). A violin plot of the top-down EC in the **HV** dataset shows higher (more excitatory) connectivity when TMS was delivered during alpha phase bins 3 and 4 (bin centered at $\pi/4$ and $3\pi/4$, respectively, Fig. 3B, left), while a plot of intrinsic (self) sgACC connection in the **MDD** dataset shows TMS is excitatory (less inhibitory) when delivered during phase bin 1 ($-3\pi/4$) relative to the other phase bins (Fig. 3B, right). Note the self-connections are unitless log scaling parameters that scale (multiply up or down) the default connection strength of −0.5Hz, so the more negative the self-connection parameter, the less inhibited the region. Note also that the MDD group data is included out of convenience to test generalizability of the findings in HV, and that we are not interested in the differences between HV vs. MDD per se. Any differences observed in the best fitting group DCMs (Fig. 3) should be interpreted with caution.

The results presented in Fig. 3B reflect models with mean centered input matrix *U* (see Ref. [33]), where the inputs are TMS pulse onsets with zero duration during the four conditions (phase bins). According to Ref. [33] this can increase the model evidence, by enabling the connectivity parameters to stay nearer to their prior expectation (of zero) during model fitting. It also means the parameters in matrix *A* represent the average effective connectivity across experimental conditions. Our primary analysis mean centered the inputs since we were mainly interested in testing for differences in connectivity strengths across the four TMS phase bins.

We also examined the effects of not mean centering the inputs as we were interested in estimating the effects of TMS modulation on connectivity, in general, relative to the implicit baseline (i.e. periods in between TMS pulses). This also allowed us to further explore sgACC-DLFPC feedback loop dynamics by estimating effective connectivity during the baseline periods (in between TMS stimulation). Results from these models are presented in SI Figure S2. When the input matrix *U* was not mean centered, the extrinsic (top-down and bottom-up) connectivity strengths no longer contributed significantly to the model fit. In these models, TMS modulated intrinsic (self) connections of DLPFC and sgACC, while sgACC intrinsic connectivity was modulated by phase bin (see SI Figure S2). The most consistent finding across both sets of models (mean-centered and non-mean centered input matrices *U*) was that models in which TMS modulated intrinsic sgACC connectivity had the best model fits, and that the intrinsic sgACC connectivity strengths showed a phase-dependent effect.

3.3. fMRI BOLD activation of the rACC depends on EEG alpha phase at TMS pulse onset in

3.3.1. MDD patients

In addition to FC with DLPFC, anterior cingulate cortex activity has been proposed as a prognostic marker of depression treatment outcomes based on deep brain stimulation and task fMRI studies [34]. Our secondary statistical analyses therefore tested whether TMS-evoked ACC activity depends on EEG prefrontal alpha phase. When applying conventional ROI analysis of TMS-evoked ACC fMRI BOLD activation, no effect of phase bin was detected in any of the ROIs in either dataset (corrected $p > 0.2$, see SI S.2 and Figure S6 for TMS-evoked BOLD signal averaged over subjects and runs for each phase bin). To overcome limitations of averaging responses within phase bin, a Generalized Additive Mixed Model (GAMM, see SI S.1.5.5) was applied which allows the use of smooth nonlinear functions to detect (continuous) relationships between alpha phase and ACC fMRI BOLD activation. The approach is more sensitive in detecting such non-linear relationships since it provides a smooth fitting across alpha phase (i.e., avoids binning of the alpha phases). Table 1 shows the main effect of phase and phase by region interactions, and the approximate significance of smooth terms based on alpha phase (φ_α). In the **HV** dataset (N = 11), we did not detect a significant main effect for phase-dependent BOLD activation across the 3 ACC subregions ($f(\varphi_\alpha)$, $p = 0.246$) and there was no difference between the three regions ($p > 0.05$). In the **MDD** dataset (N = 17), the phase-dependent BOLD activation was significant in rACC ($f(\varphi_\alpha)$:rostral, $p = 0.017$ uncorrected). Applying Fisher's method to combine p-values across results from both datasets suggested an overall phase-dependent BOLD activation effect within rACC ($p = 0.040$). The results with respect to brain regions in the **MDD** group are summarized in Fig. 4 (left panel), while Fig. 4 (right panel) plots the corresponding normalized BOLD signal (BOLD*nor*) differences between $-\pi$ and π in rACC. Table 2 shows results of significance tests for the parametric coefficients of the GAMM model for both **HV** and **MDD** groups. The results show that in the **HV** group, there is no significant difference in maximum BOLD activation across regions (rostral-dorsal: $p = 0.3875$, subgenual-dorsal: $p = 0.2225$), while in the **MDD** group, there is a significant difference in maximum BOLD activation between regions (rostral-dorsal: $p = 0.0371$, rostral-dorsal: $p = 0.0274$).

Table 1
GAMM results in **HV** and **MDD** datasets and approximate significance of smooth terms. (**) indicates significance at the 99% confidence level; (*) indicates significance at the 95% confidence level; (.) indicates significance at the 90% confidence level.

HV	*p*-value	MDD	*p*-value
f(*sub*,$\varphi\alpha$)	0.0726 (.)	f(*sub*,$\varphi\alpha$)	0.009 (**)
f($\varphi\alpha$)	0.246	f($\varphi\alpha$)	0.386
f($\varphi\alpha$):dorsal	0.998	f($\varphi\alpha$):dorsal	0.475
f($\varphi\alpha$):rostral	0.393	f($\varphi\alpha$):rostral	0.017 (*)
f($\varphi\alpha$):subgenual	0.219	f($\varphi\alpha$):subgenual	0.744

4. DISCUSSION

In this study, we used our recently developed integrated fET instrument capable of acquiring simultaneous EEG-fMRI while delivering noninvasive single pulse TMS, and found that TMS applied to DLPFC modulates the region's (fMRI-derived) connectivity with ACC in a way that depends on prefrontal EEG alpha phase. In both the **HV** and **MDD** datasets, phase dependent functional and effective connectivity with the left DLPFC was seen in sgACC. The most consistent phase-dependent effect, observed in both datasets, was DLPFC-sgACC functional connectivity following single pulse TMS. The EEG F3 DLPFC-sgACC TMS-evoked functional connectivity straddles zero and is overall weakly negative, consistent with resting state studies that found EEGF3 DLPFC-sgACC functional connectivity is the least (weakly) negative ($r \approx -0.05$) compared to other TMS stimulation sites in the DLPFC (i.e. see Fig. 1 in Ref. [19]). With the GAMM model, we also observed phase dependent activation in the **MDD** group, such that TMS-evoked BOLD responses in the rACC were lowest when TMS pulses were synchronized nearer to the peak of the frontal alpha oscillation.

The primary hypothesis tested in the current study is whether the prefrontal alpha phase at TMS pulse onset is significantly associated with ACC activation or ACC functional connectivity (FC) with DLPFC. The 'control' condition (null hypothesis) is no association between these measures and prefrontal alpha phase, which we tested using both parametric and non-parametric (permutation based) approaches. The strongest effects were observed for sgACC-DLPFC functional connectivity (omnibus F cluster-extent corrected $p = 0.0035$ and $p = 0.0085$ in each dataset using FSL randomise, respectively, with a Fisher combined $p = 0.00035$ across both datasets). This finding survives $p < 0.05$ Bonferroni correction which is the most conservative correction for multiple comparisons when correcting for the total number of independent tests (n = 11) across the 5 ACC ROIs which are comprised of 5 conventional GLM activation and 5 PPI models using SVC, and 1 GAMM activation model which included all ROIs in the same model. Moreover,

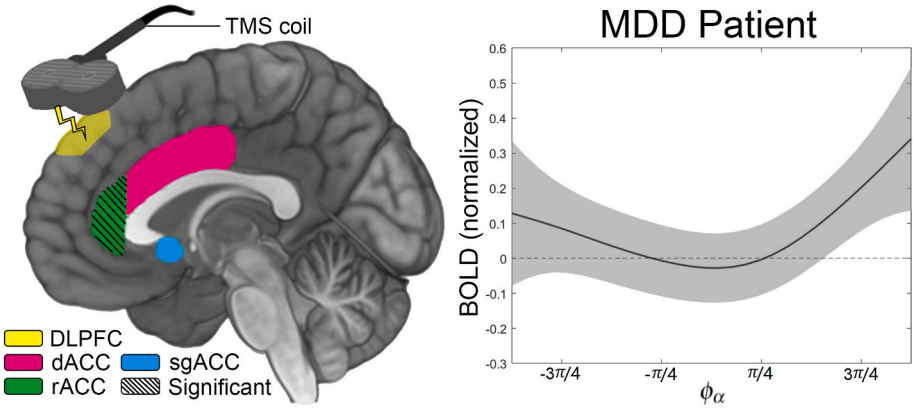

Fig. 4. TMS-evoked BOLD activation in rostral ACC (rACC) is correlated with alpha phase at TMS pulse onset in the **MDD** dataset only. The phase-dependent BOLD activation is significant (diagonal stripes) in rACC (left panel). The right panel plots the BOLD activation (curves fitted from the GAMM models) against alpha phase. The results show that in the **MDD** dataset, the TMS-evoked BOLD response in the rACC (i.e. the normalized BOLD activation $BOLD_{nor}$, see SI S.1.5.5) is related to the corresponding alpha phase φ_α at which the TMS pulse is triggered (see Table 1, random effects on the subject level are not plotted).

Table 2
GAMM results in **HV** and **MDD** datasets and approximate significance of parametric terms. (**) indicates significance at the 99% confidence level; (*) indicates significance at the 95% confidence level; (.) indicates significance at the 90% confidence level.

HV	*p*-value	MDD	*p*-value
(Intercept)	0.0285 (*)	(Intercept)	5.87e-08 (***)
rostral	0.3875	rostral	0.0371 (*)
subgenual	0.2225	subgenual	0.0274 (*)

the DLPFC-sgACC FC show a similar pattern relative to phase in both HV and MDD datasets (i.e. higher FC during the rising, and lower FC during the falling, phase of prefrontal alpha), which increase confidence that these results reflect a real physiological, rather than artifactual, effect.

An effective connectivity analysis suggests that in **HV** there is an excitatory/inhibitory feedback loop between DLPFC and sgACC and that TMS has a phase dependent effect on the top-down connection. The effective connectivity analysis in the **MDD** dataset suggests: (1) the DLPFC-sgACC feedback loop is purely positive (excitatory connections) and reflects hyperactivation of sgACC/ACC; (2) the phase dependent effect of TMS is not seen in the top-down connection (as in the **HV** group), though there are phase-dependent effects on sgACC intrinsic connectivity. The observed functional and effective connectivity effects could be mediated via indirect structural connections to sgACC or via direct structural connections between DLPFC and sgACC. Tract tracing studies in primates have shown sparse structural connections between left posterior DLPFC and sgACC [35]. Note that we detected significant phase-dependent differences in TMS-evoked top-down DLPFC-sgACC effective connectivity strengths in HV and sgACC intrinsic connectivity strength differences in MDD even though the sample sizes (N = 11 and N = 17) in each group are smaller than previously recommended sample sizes (approximately 20) for Dynamic Causal Modeling [36]. This is likely owing to the fact that participants each had more than 30 min of scan data (~240 TMS trials total per subject). Previous research suggests n = 25 events per condition are sufficient for event-related fMRI designs and minimal gains are obtained after 40 events [37,38]. Our design includes 240 events per subject, leaving 60 events per condition per subject, which is likely well-powered to detect phase effects.

A study of single unit recordings in V1 of awake monkeys estimated spike probability as a function of gamma phase LFP, and found highest (lowest) spike probabilities during the peak (trough) of the gamma wave [1,39]. Our GAMM results followed a similar pattern, whereby fMRI BOLD signal was lowest for TMS pulses timed nearest to the peak of the alpha wave. However, functional and effective connectivity did not line up with the peaks and troughs of the EEG alpha wave. Rather, these measures lined up with the slope of the EEG alpha wave, whereby functional connectivity was highest (positive) for TMS pulses on the upward slope of the alpha wave, and lowest (negative) for TMS pulses during the downward slope of the alpha wave. The DCM analysis (in **HV**) suggested TMS-evoked top-down DLPFC-sgACC EC was negative (inhibitory) for TMS pulses on the upward slope of the alpha wave, and positive (excitatory) for TMS delivered during the downward slope of the alpha wave. The results are consistent with a previous study that found neocortical activity converged to a preferred phase of 45° in response to exogenous or endogenous electrical fields [40]. The findings suggest that the rate of change of, rather than absolute, membrane potential of cortical neuronal populations is a determining factor in TMS-evoked downstream DLPFC signaling, and that the "rising" and "falling" phases of alpha are when cortical neuronal populations are most "primed" to propagate signals to sgACC.

4.1. Clinical application in depression

The effects observed here have potentially important implications for clinical applications involving TMS. Depression involves distributed cortico-limbic networks, with anterior cingulate cortex (ACC) playing an important role in the etiology and treatment of the disorder [41–43]. TMS targeting left DLPFC is currently used for treatment of medication-resistant depression [44–47], yielding remission rates of 28–53% [48]. Understanding the mechanisms of rTMS and increasing the efficacy of rTMS is an important area of research.

The anti-depressant effects of TMS are likely mediated by connectivity between DLFPC and ACC, and the modulation of ACC activity [19,49,50]. Previous studies have examined TMS efficacy based on spatial location of stimulation within DLPFC and find that anterolateral DLPFC regions lead to better outcomes perhaps because they are more negatively functionally connected with sgACC [21]. Additionally, several groups have reported that alpha-band oscillations are associated with both activation and inhibition across and within different functional networks [5,6,51]. Therefore, by controlling or targeting the phase of alpha rhythms, we could potentially activate or inhibit brain excitability within certain networks that are phase-dependent.

Our study finds that TMS-evoked brain excitability or functional connectivity can be indexed by phase. This suggests that deep targets may be more efficiently engaged by TMS via optimizing TMS delivery based on these indeces (e.g., alpha phase) of excitability or functional connectivity, which in turn could improve TMS treatment efficacy. In other words, TMS treatment could be improved by synchronizing the timing of TMS stimulation with the brain's internal EEG rhythms in way that maximizes excitability or functional connectivity with deep therapeutic targets [8,17,52].

The full clinical results of the background clinical trial are in a different manuscript under review. This clinical trial showed that

synchronizing prefrontal TMS with a patient's prefrontal alpha frequency in a blinded clinical trial is possible and produces progressive EEG entrainment in synchronized patients only. In this small clinical trial, there was no difference in overall clinical response between synchronized and not synchronized patients, all treated at their individual alpha frequency (IAF). A secondary analysis showed that only in the synchronized (vs. non-synchronized) TMS treatment patient group, the consistency of the entrained phase across sessions was significantly associated with response outcome.

Some prior studies have observed that prefrontal alpha frequency matching might improve TMS depression outcomes [53,54]. They have not tested for EEG synchronization while also matching individual alpha frequency. In our study, both arms were delivered at the IAF and we are only testing whether EEG phase matching caused EEG changes and predicted clinical outcome. Due to budget limitations and blinding issues, we were not able to include another arm of conventional TMS at a fixed 10 Hz frequency.

Since the initial design and launch of this trial, there have been other advances with TMS for depression that have likely improved overall efficacy and speed of response. These involved individualizing the coil placement or accelerating the number of pulses within a given week [55,56]. At this point it is unclear which of these advances, or both, are responsible for the increased efficacy. We used conventional coil placement (F3) and only 5 sessions/week. However, our advances with phase synchronization might ultimately be added to the other innovations and have additional increases in efficacy. That is, this issue of EEG synchronization is likely clinically important regardless of which other TMS methods are used.

4.2. Limitations

There are some limitations when interpreting the findings in our paper more broadly. First, how we extracted the alpha oscillation and its phase from prefrontal EEG could be suboptimal. One reason for that is the relatively complex EEG-fMRI-TMS apparatus we used in this challenging recording environment. The apparatus enabled us to perform the tri-modal experiment to investigate our research question, but limited us in the number of available EEG electrodes and thus our choice of spatial filtering methods. Though we record EEG such that adjacent electrodes are recorded as a hard-wired bi-polar pair, others have found using more conventional recording techniques that associations between alpha and 10Hz TMS are seen using an average reference and not linked ears [53,54]. This raises the possibility that using an average reference may have yielded different results than the mastoid reference used here. We did not further study alternative spatial filters to extract the signal of interest. However, this is an area where we plan to conduct additional investigations in future research. Another potential limitation of our study that may have weakened observed effects is that the custom EEG amplifier that we used for this complex recording environment was not designed to recover quasi instantly as some commercially available non-fMRI compatible amplifiers do.

5. Conclusion

Using simultaneous fMRI-EEG-TMS (fET) we find that the timing of TMS relative to prefrontal alpha phase results in differential sgACC functional and effective connectivity with the left DLPFC stimulation site. TMS applied during the rising phase of the alpha wave has an inhibitory effect on sgACC, while TMS during the falling phase has an excitatory effect. In addition, we find evidence for EEG alpha dependent BOLD activation in the rACC, at least in the **MDD** group. The findings demonstrate that prefrontal alpha wave activity modulates top-down influences from executive brain regions to anterior cingulate. Moreover, they suggest potential clinical applications whereby TMS that is timed to internal brain rhythms could lead to more effective rTMS and improve clinical outcomes. Future work should examine whether rTMS that is synchronized to alpha wave activity can improve clinical outcomes.

CRediT authorship contribution statement

Spiro P. Pantazatos: Formal analysis, Visualization, Writing – original draft. **James R. Mclntosh:** Software, Validation, Visualization, Writing – review & editing. **Golbarg T. Saber:** Investigation, Methodology, Data curation. **Xiaoxiao Sun:** Formal analysis, Visualization, Writing – original draft. **Jayce Doose:** Investigation, Methodology, Data curation, Project administration. **Josef Faller:** Methodology, Software, Writing – review & editing. **Yida Lin:** Software, Investigation. **Joshua B. Teves:** Software, Investigation. **Aidan Blankenship:** Project administration, Data curation. **Sarah Huffman:** Project administration, Investigation. **Robin I. Goldman:** Methodology, Writing – review & editing. **Mark S. George:** Conceptualization, Methodology, Writing – review & editing, Funding acquisition, Supervision. **Paul Sajda:** Conceptualization, Methodology, Writing – review & editing, Funding acquisition, Supervision. **Truman R. Brown:** Conceptualization, Methodology, Writing – review & editing, Funding acquisition, Supervision.

Declaration of competing interest

The authors declare the following financial interests/personal relationships which may be considered as potential competing interests: Authors SPP, JRM, GTS, XS, JD, JF, YL, JBT, AB, RIG, SH, TRB have no relevant conflicts of interest to report. Dr. George reports being a paid consultant to Sooma Medical (tDCS) and Neuralief (VNS, trigeminal), and being an unpaid consultant to Mecta (ECT), Brainsway (TMS), Magnus Medical (TMS), Magstim (TMS), Brainsonix (ultrasound). He was a paid DSMB member for Microtransponder (VNS). He has loaned research equipment from MECTA, and Magstim. He has held research grants from Brainsway, Neuralief, Livanova. Dr. Sajda reports being a paid consultant for Optios Inc. and OpenBCI LLC.

Acknowledgments

This work was funded by the National Institute of Mental Health (MH106775) and a Vannevar Bush Faculty Fellowship from the US Department of Defense (N00014-20-1-2027). We would like to thank Daniel Cook for his help with initial data collection with closed-loop EEG-rTMS. We would like to thank Michael Milici for his help with building the safety circuit box and ActiChamp testing. We would like to thank DeeAnn Guo for her help with ActiChamp testing and initial EEG data collection.

Appendix A. Supplementary data

Supplementary data to this article can be found online at https://doi.org/10.1016/j.brs.2023.05.007.

References

[1] Fries Pascal. Rhythms for cognition: communication through coherence. Neuron 2015;88(1):220–35.
[2] Scheeringa René, Fries Pascal. Cortical layers, rhythms and bold signals. Neuroimage 2019;197:689–98.
[3] Womelsdorf Thilo, Mathijs Schoffelen Jan, Oostenveld Robert, Singer Wolf, Desimone Robert, Engel Andreas K, Fries Pascal. Modulation of neuronal interactions through neuronal synchronization. Science 2007;316(5831):1609–12.
[4] Peters Judith C, Reithler Joel, Schuhmann Teresa, Graaf Tom De, Uludağ Kâmil, Goebel Rainer, Sack Alexander T. On the feasibility of concurrent human TMS-EEG-fMRI measurements. J Neurophysiol 2013;109(4):1214–27.
[5] Klimesch Wolfgang. Alpha-band oscillations, attention, and controlled access to stored information. Trends Cognit Sci 2012;16(12):606–17.
[6] Sadaghiani Sepideh, Scheeringa René, Lehongre Katia, Morillon Benjamin, Lise Giraud Anne, d'Esposito Mark, Kleinschmidt Andreas. Alpha-band phase synchrony is related to activity in the fronto- parietal adaptive control network. J Neurosci 2012;32(41):14305–10.

[7] Dosenbach Nico UF, Fair Damien A, Miezin Francis M, Cohen Alexander L, Wenger Kristin K, Dosenbach Ronny AT, Fox Michael D, Snyder Abraham Z, Vincent Justin L, Raichle Marcus E, et al. Distinct brain networks for adaptive and stable task control in humans. Proc Natl Acad Sci USA 2007;104(26):11073–8.

[8] Faller Josef, Doose Jayce, Sun Xiaoxiao, Mclntosh James R, Saber Golbarg T, Lin Yida, Teves Joshua B, Blankenship Aidan, Huffman Sarah, Goldman Robin I, et al. Daily prefrontal closed-loop repetitive transcranial magnetic stimulation (rTMS) produces progressive eeg quasi-alpha phase entrainment in depressed adults. Brain Stimul 2022;15(2):458–71.

[9] Busch Niko A, Dubois Julien, VanRullen Rufin. The phase of ongoing eeg oscillations predicts visual perception. J Neurosci 2009;29(24):7869–76.

[10] Milton Alex, Pleydell-Pearce Christopher W. The phase of pre-stimulus alpha oscillations influences the visual perception of stimulus timing. Neuroimage 2016; 133:53–61.

[11] Ronconi Luca, Busch Niko A, Melcher David. Alpha-band sensory entrainment alters the duration of temporal windows in visual perception. Sci Rep 2018;8(1): 1–10.

[12] Ferreri Florinda, Vecchio Fabrizio, Ponzo David, Pasqualetti Patrizio, Maria Rossini Paolo. Time- varying coupling of eeg oscillations predicts excitability fluctuations in the primary motor cortex as reflected by motor evoked potentials amplitude: an eeg-tms study. Hum Brain Mapp 2014;35(5):1969–80.

[13] Fuggetta Giorgio, Fiaschi Antonio, Manganotti Paolo. Modulation of cortical oscillatory activities induced by varying single-pulse transcranial magnetic stimulation intensity over the left primary motor area: a combined eeg and tms study. Neuroimage 2005;27(4):896–908.

[14] Keil Julian, Jana Timm, SanMiguel Iria, Schulz Hannah, Jonas Obleser, Schö nwiesner Marc. Cor- tical brain states and corticospinal synchronization influence tms-evoked motor potentials. J Neurophysiol 2014;111(3):513–9.

[15] Zrenner Christoph, Desideri Debora, Belardinelli Paolo, Ziemann Ulf. Real-time eeg-defined excitability states determine efficacy of tms-induced plasticity in human motor cortex. Brain Stimul 2018;11(2):374–89.

[16] Walz Jennifer M, Goldman Robin I, Carapezza Michael, Jordan Muraskin, Brown Truman R, Paul Sajda. Prestimulus eeg alpha oscillations modulate task-related fmri bold responses to auditory stimuli. Neuroimage 2015;113:153–63.

[17] Faller Josef, Lin Y, Doose J, Saber GT, McIntosh JR, Teves JB, Goldman Robin I, George MS, Paul Sajda, Brown Truman R. An eeg-fmri-tms instrument to investigate bold response to eeg guided stimulation. In: 2019 9th international IEEE/EMBS conference on neural engineering (NER). IEEE; 2019. p. 1054–7.

[18] Anderson Rodney J, Hoy Kate E, Daskalakis Zafiris J, Fitzgerald Paul B. Repetitive transcranial magnetic stimulation for treatment resistant depression: Re-establishing connections. Clin Neurophysiol 2016;127(11):3394–405.

[19] Fox Michael D, Buckner Randy L, White Matthew P, Greicius Michael D, Pascual-Leone Alvaro. Efficacy of transcranial magnetic stimulation targets for depression is related to intrinsic functional connec- tivity with the subgenual cingulate. Biol Psychiatr October 2012;72(7):595–603. https://doi.org/10.1016/j.biopsych.2012.04.028. ISSN 1873-2402.

[20] Johansen-Berg H, Gutman DA, Behrens TEJ, Matthews PM, Rushworth MFS, Katz E, Lozano AM, Mayberg HS. Anatomical connectivity of the subgenual cingulate region targeted with deep brain stimulation for treatment-resistant depression. Cerebr Cortex 2008;18(6):1374–83.

[21] Weigand Anne, Horn Andreas, Caballero Ruth, Cooke Danielle, Stern Adam P, Taylor Stephan F, Press Daniel, Pascual-Leone Alvaro, Michael D Fox. Prospective validation that subgenual connectivity predicts antidepressant efficacy of transcranial magnetic stimulation sites. Biol Psychiatr July 2018;84(1):28–37. https://doi.org/10.1016/j.biopsych.2017.10.028. ISSN 0006-3223, http://www.sciencedirect.com/science/article/pii/S0006322317321583.

[22] Friston KJ, Buechel C, Fink GR, Morris J, Rolls E, Dolan RJ. Psychophysiological and modulatory interactions in neuroimaging. Neuroimage 1997;6(3):218–29.

[23] McLaren DG, Ries ML, Xu G, Johnson SC. A generalized form of context-dependent psychophysio- logical interactions (gPPI): a comparison to standard approaches. Neuroimage 2012;61(4):1277–86.

[24] Paul Sajda, Goldman Robin I, Dyrholm Mads, Brown Truman R. Signal processing and machine learning for single-trial analysis of simultaneously acquired eeg and fmri. In: Statistical signal processing for neuroscience and neurotechnology. Elsevier; 2010. p. 311–34.

[25] Robin I Goldman John M Stern, Engel Jr Jerome, Cohen Mark S. Acquiring simultaneous eeg and functional mri. Clin Neurophysiol 2000;111(11):1974–80.

[26] Beam William, Borckardt Jeffrey J, Reeves Scott T, George Mark S. An efficient and accurate new method for locating the f3 position for prefrontal tms applications. Brain Stimul 2009;2(1):50–4.

[27] McClintock Shawn M, Reti Irving M, Carpenter Linda L, McDonald William M, Dubin Marc, Taylor Stephan F, Cook Ian A, John O, Husain Mustafa M, Wall Christopher, et al. Consensus recommendations for the clinical application of repetitive transcranial magnetic stimulation (rtms) in the treatment of depression. J Clin Psychiatr 2017;79(1):3651.

[28] Herwig Uwe, Satrapi Peyman, Schö nfeldt-Lecuona Carlos. Using the international 10-20 eeg system for positioning of transcranial magnetic stimulation. Brain Topogr 2003;16(2):95–9.

[29] McIntosh James R, Paul Sajda. Estimation of phase in eeg rhythms for real-time applications. J Neural Eng 2020;17(3):034002.

[30] Miles Wischnewski, Haigh Zachary J, Shirinpour Sina, Alekseichuk Ivan, Alexander Opitz. The phase of sensorimotor mu and beta oscillations has the opposite effect on corticospinal excitability. bioRxiv; 2022.

[31] Eklund A, Nichols TE, Knutsson H. Cluster failure: why fMRI inferences for spatial extent have inflated false-positive rates. Proc. Natl. Acad. Sci. U.S.A 2016;113(28): 7900–5.

[32] Friston Karl J, Litvak Vladimir, Oswal Ashwini, Razi Adeel, Stephan Klaas E, Bernadette CM Van Wijk, Ziegler Gabriel, Peter Zeidman. Bayesian model reduction and empirical bayes for group (dcm) studies. Neuroimage 2016;128: 413–31.

[33] Peter Zeidman, Jafarian Amirhossein, Corbin Nadège, Seghier Mohamed L, Razi Adeel, Price Cathy J, Friston Karl J. A guide to group effective connectivity analysis, part 1: first level analysis with dcm for fmri. Neuroimage 2019;200: 174–90.

[34] Siegle Greg J, Thompson Wesley K, Collier Amanda, Berman Susan R, Feldmiller Joshua, Thase Michael E, Friedman Edward S. Toward clinically useful neuroimaging in depression treatment: prognostic utility of subgenual cingulate activity for determining depression outcome in cognitive therapy across studies, scanners, and patient characteristics. Arch Gen Psychiatr 2012;69(9):913–24.

[35] Joyce Mary Kate P, Barbas Helen. Cortical connections position primate area 25 as a keystone for interoception, emotion, and memory. J Neurosci 2018;38(7): 1677–98.

[36] Goulden Nia, Elliott Rebecca, Suckling John, Williams Stephen Ross, Deakin John Francis William, McKie Shane. Sample size estimation for comparing parameters using dynamic causal modeling. Brain Connect 2012;2(2):80–90.

[37] Huettel Scott A, McCarthy Gregory. The effects of single-trial averaging upon the spatial extent of fmri activation. Neuroreport 2001;12(11):2411–6.

[38] Murphy Kevin, Garavan Hugh. Deriving the optimal number of events for an event-related fmri study based on the spatial extent of activation. Neuroimage 2005;27 (4):771–7.

[39] Womelsdorf Thilo, Lima Bruss, Vinck Martin, Oostenveld Robert, Singer Wolf, Neuenschwander Sergio, Fries Pascal. Orientation selectivity and noise correlation in awake monkey area v1 are modulated by the gamma cycle. Proc Natl Acad Sci USA 2012;109(11):4302–7.

[40] Flavio Frö hlich, McCormick David A. Endogenous electric fields may guide neocortical network activity. Neuron 2010;67(1):129–43.

[41] Diego A Pizzagalli. Frontocingulate dysfunction in depression: toward biomarkers of treatment response. Neuropsychopharmacology 2011;36(1):183–206.

[42] Mulders Peter C, van Eijndhoven Philip F, Schene Aart H, Beckmann Christian F, Tendolkar Indira. Resting-state functional connectivity in major depressive disorder: a review. Neurosci Biobehav Rev 2015;56:330–44.

[43] Greicius Michael D, Flores Benjamin H, Menon Vinod, Glover Gary H, Solvason Hugh B, Kenna Heather, Reiss Allan L, Schatzberg Alan F. Resting-state functional connectivity in major depression: abnormally increased contributions from subgenual cingulate cortex and thalamus. Biol Psychiatr 2007;62(5):429–37.

[44] George Mark S, Wassermann Eric M, Williams Wendol A, Callahan Ann, Ketter Terence A, Basser Peter, Hallett Mark, Post Robert M. Daily repetitive transcranial magnetic stimulation (rtms) improves mood in depression. Neuroreport: Int J Rapid Commun Res Neurosci 1995.

[45] Pascual-Leone Alvaro, Rubio Belen, Pallardó Federico, Dolores Catalá Maria. Rapid-rate transcranial magnetic stimulation of left dorsolateral prefrontal cortex in drug-resistant depression. Lancet 1996;348(9022):233–7.

[46] O'Reardon John P, Brent Solvason H, Janicak Philip G, Sampson Shirlene, Keith E Isenberg, Nahas Ziad, McDonald William M, Avery David, Fitzgerald Paul B, Loo Colleen, et al. Efficacy and safety of transcranial magnetic stimulation in the acute treatment of major depression: a multisite randomized controlled trial. Biol Psychiatr 2007;62(11):1208–16.

[47] Frank Padberg, George Mark S. Repetitive transcranial magnetic stimulation of the prefrontal cortex in depression. Exp Neurol 2009;219(1):2–13.

[48] Carpenter LindaL, Aaronson ScottT, Hutton Todd M, Mina Miriam, Pages Kenneth, Verdoliva Sarah, West W Scott, Sackeim HaroldA. Comparison of clinical outcomes with two transcranial magnetic stimulation treatment protocols for major depressive disorder. Brain Stimul 2021;14(1):173–80.

[49] Kito Shinsuke, Fujita Kenichi, Koga Yoshihiko. Changes in regional cerebral blood flow after repetitive transcranial magnetic stimulation of the left dorsolateral prefrontal cortex in treatment-resistant depression. J Neuropsychiatry Clin Neurosci 2008;20(1):74–80.

[50] Caspers Julian, Mathys Christian, Hoffstaedter Felix, Sudmeyer Martin, Cieslik Edna C, Rubbert Christian, Hartmann Christian J, Eickhoff Claudia R, Reetz Kathrin, Grefkes Christian, et al. Differential functional connectivity alterations of two subdivisions within the right dlpfc in Parkinson's disease. Front Hum Neurosci 2017;11:288.

[51] Foxe John J, Snyder Adam C. The role of alpha-band brain oscillations as a sensory suppression mechanism during selective attention. Front Psychol 2011;2:154.

[52] George M, Saber G, McIntosh J, Doose J, Faller J, Lin Y, Moss H, Goldman R, Sajda P, Brown T. Combined tms-eeg-fmri. the level of tms-evoked activation in anterior cingulate cortex depends on timing of tms delivery relative to frontal alpha phase. Brain Stimul: Basic Translat Clin Res Neuromodulat 2019;12(2):580.

[53] Roelofs Charlotte L, Krepel Noralie, Corlier Juliana, Carpenter Linda L, Fitzgerald Paul B, Daskalakis Zafiris J, Tendolkar Indira, Wilson Andrew, Downar Jonathan, Bailey Neil W, et al. Individual alpha frequency proximity associated with repetitive transcranial magnetic stimulation outcome: an independent replication study from the icon-db consortium. Clin Neurophysiol 2021;132(2):643–9.

[54] Corlier Juliana, Carpenter Linda L, Wilson Andrew C, Tirrell Eric, Gobin A Polly, Kavanaugh Brian, Leuchter Andrew F. The relationship between individual alpha

peak frequency and clinical outcome with repetitive transcranial magnetic stimulation (rtms) treatment of major depressive disorder (mdd). Brain Stimul 2019;12(6):1572–8.

[55] Cole Eleanor J, Stimpson Katy H, Bentzley Brandon S, Gulser Merve, Cherian Kirsten, Tischler Claudia, Nejad Romina, Pankow Heather, Choi Elizabeth, Aaron Haley, et al. Stanford accelerated intelligent neuromodulation therapy for treatment-resistant depression. Am J Psychiatr 2020;177(8):716–26.

[56] Cole Eleanor J, Phillips Angela L, Bentzley Brandon S, Stimpson Katy H, Nejad Romina, Barmak Fahim, Veerapal Clive, Khan Naushaba, Cherian Kirsten, Felber Emily, et al. Stanford neuromodulation therapy (snt): a double-blind randomized controlled trial. Am J Psychiatr 2022;179(2):132–41.